ACS APPLIED MATERIALS & INTERFACES

Research Article

www.acsami.org

Carbon Dot Loading and TiO_2 Nanorod Length Dependence of Photoelectrochemical Properties in Carbon Dot/TiO_2 Nanorod Array Nanocomposites

Juncao Bian,[†] Chao Huang,[†] Lingyun Wang,[‡] TakFu Hung,[†] Walid A. Daoud,[‡] and Ruiqin Zhang*[,†]

[†]Department of Physics and Materials Science and Centre for Functional Photonics (CFP), City University of Hong Kong, Kowloon, Hong Kong SAR, China

[‡]School of Energy and Environment, City University of Hong Kong, Kowloon, Hong Kong SAR, China

Supporting Information

ABSTRACT: Photoelectrochemcial (PEC) properties of TiO_2 nanorod arrays (TNRA) have been extensively investigated as they are photostable and cost-effective. However, due to the wide band gap, only the UV part of solar light can be employed by TiO_2. To enhance the photoresponse of TNRA in the visible range, carbon dots (C dots) were applied as green sensitizer in this work by investigating the effects of C dot loading and length of TiO_2 nanorod on the PEC properties of TNRA/C dot nanocomposites. As the C dot loading increases, the photocurrent density of the nanocomposites was enhanced and reached a maximum when the concentration of the C dots was 0.4 mg/mL. A further increase in the C dot concentration decreased the photocurrent, which might be caused by the surface aggregation of C dots. A compromise existed between charge transport and charge collection as the length of TiO_2 nanorod increased. The incident photon to current conversion efficiency (IPCE) of the TNRA/C dot nanocomposites in the visible range was up to 1.2−3.4%. This work can serve as guidance for fabrication of highly efficient photoanode for PEC cells based on C dots.

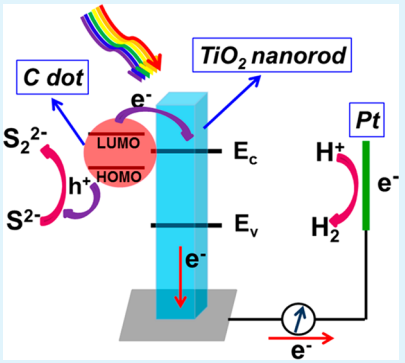

KEYWORDS: *carbon dots, TiO_2 nanorod arrays, photoanode, loading, length*

1. INTRODUCTION

Since the pioneering work of Honda and Fujishima on water splitting with Pt−TiO_2 nanocomposites, photoelectrochemical (PEC) properties of TiO_2 have been extensively investigated since it is photostable, nontoxic, cost-effective, and abundant.[1−7] Among the various TiO_2 nanostructures, one-dimensional TiO_2 including nanorods, nanotubes, and nanowires have been confirmed to be superior to other dimensional TiO_2 nanostructures as they can enhance the charge separation and offer a pathway for oriented charge carrier transport.[8−11] However, the grain boundaries in polycrystalline TiO_2 nanowires or nanotubes cause electron scattering or trapping, which limit their application in optoelectronics.[8,10] In contrast, single crystal TiO_2 nanorods have less defect related barriers blocking the charge carrier transport,[5,9] and the length of nanorods is a key factor influencing the charge collection efficiency. Recently, Yang and co-workers reported that, with increasing the length of the single crystalline rutile TiO_2 nanorods to about 1.8 μm, the photocurrent density was close to the maximum.[5]

On the other hand, bulk TiO_2, with the band gaps of 3.0 eV (in rutile phase) and 3.2 eV (in anatase phase), can only absorb the light in the UV part, which makes up less than 4% of the total solar light reaching the surface of earth.[4] To enhance the light absorption ability of TiO_2 in the visible region, various routes such as doping,[3,7,12,13] using surface plasmons of Au[14,15] and Ag,[16] and coupling with narrow-band gap semiconductors[17−20] and dyes[21] were employed. Recently, carbon dots (C dots) have become a star in the area of quantum dots (QDs) as they are of low-toxicity and eco-friendly compared with the traditional toxic metal-based QDs.[22−28] With many carboxylic acid moieties on their surface, C dots can be well dispersed in water and are suitable for subsequent functionalization with various organic and inorganic species.[22,25,26] The C dots typically exhibit size and excitation wavelength dependent photoluminescence (PL) properties and have great potential in bioimaging,[26] light-emitting diodes (LEDs),[29] solar cells,[30] catalysis,[24,31−34] and PEC cells.[35]

In this work, C dots were used as sensitizer to enhance the PEC performance of TiO_2 nanorods arrays (TNRA). It is well recognized that photoabsorption, charge transport in semiconductor, and charge separation are three main factors influencing the efficiency of PEC cells. Hence, the effect of C dot loading on the surface of TNRA was investigated to optimize the light absorption and charge separation properties, and the length of TNRA was investigated to optimize the PEC performance from the aspect of charge transport. It was found that C dots can enhance the photoresponse of TNRA in the

Received: December 23, 2013
Accepted: March 6, 2014
Published: March 6, 2014

   dx.doi.org/10.1021/am4059183 | ACS Appl. Mater. Interfaces 2014, 6, 4883−4890

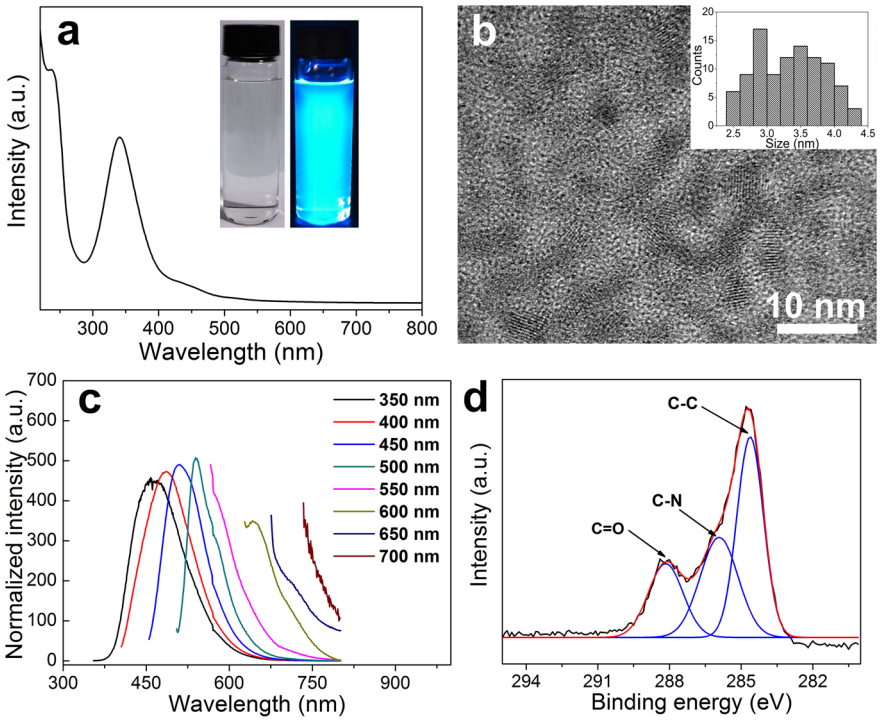

Figure 1. (a) UV–vis, (b) HRTEM image (inset: size diagram), and (c) photoluminescence spectra of C dots. (d) XPS spectrum of C dots on the surface of TNRA. Insets in (a) are the C dots solution (0.005 mg/mL) under lamplight (left) and UV light (360 nm) (right) illumination.

visible range with the incident photon to current conversion efficiency (IPCE) being more than 1%. The related mechanisms are discussed.

2. EXPERIMENTAL DETAILS

All reagents were purchased from Acros unless otherwise stated. Highly ordered single-crystal TNRA were fabricated on FTO glasses by a modified hydrothermal growth method.[9] 15 mL of concentrated HCl (37%) was mixed with 15 mL of ultrapure water (18.2 MΩ·cm), and the mixture was stirred for 5 min. Then, 0.8 mL of titanium butoxide was added. After vigorously stirring for another 5 min, 10 mL of the solution was transferred to a 23 mL Teflon liner, and precleaned FTO glass (2 × 3.3 cm^2, square resistance: < 10 Ω, Zhuhai Kaivo Optoelectronic Technology Co., Ltd.) was placed against the wall of the Teflon liner with the conducting side facing down. Then, the autoclaves were put into an oven and kept at 150 °C for different durations to obtain the TNRA with different lengths. The autoclaves were cooled down by water for 15 min. Then, the FTO glasses with TNRA were ultrasonically cleaned by ultrapure water for 5 min to remove the surface remnant.

C dots were synthesized by a hydrothermal method.[26] 1.05 g of citric acid (Sigma Aldrich) and 335 μL of ethylenediamine were dissolved in 10 mL of ultrapure water. The mixtures were vigorously stirred for 10 min. They were then transferred to a 23 mL Teflon-lined autoclave and kept in an oven (200 °C) for 5 h. After the reaction, the autoclave was cooled down by water for 15 min. Then, after dialysis (M = 1000), rotary evaporation, and freeze-drying processes, C dot powders were collected. For TNRA/C dot nanocomposites, TNRA on FTO glasses were immersed into C dot solutions with different concentrations for 20 h in the dark. Then, they were taken out, rinsed with ultrapure water, and dried off with N_2. The TNRA/C dot nanocomposites were then annealed in a rapid annealing furnace for 20 min at 200 °C under N_2 atmosphere (60 Torr).

The photoluminescence spectra of C dots were investigated by a Varian Fluorescence Spectrophotometer. Raman spectra of C dots and TNRA/C dot nanocomposites were obtained from the micro Raman system (RM 3000 Ranishaw, Laser: 514.5 nm) with confocal microscopy. The UV–vis absorption spectrum of C dots was measured on a Varian 50 Conc UV–visible spectrophotometer. UV–vis absorption spectra of TNRA/C dots were carried out on a UV–vis-NIR (UV 3600, Shimadzu) spectrophotometer equipped with integrating sphere. High resolution transmission electron microscope (HRTEM) images of C dots and TNRA/C dot nanocomposites were measured from a HRTEM (JEOL 2100F). Top-down and cross-section morphologies of TNRA were obtained from scanning electron microscopy (SEM, JEOL JSM-6335F). X-ray photoelectron spectroscopy (XPS) was performed on XPS (PHI Model 5802) with Al Kα radiation and was calibrated by C1s.

Photoelectrochemical (PEC) properties of TNRA/C dot nanocomposites were measured in a PEC cell. The photoresponse of the photoanodes were recorded by a three-electrode electrochemical workstation (CHI 760E), in which FTO supported TNRA/C dot nanocomposites, Pt wire, and Ag/AgCl were used as working electrode, counter electrode, and reference electrode, respectively. Solutions containing 0.1 M $NaSO_4$ and 0.01 M Na_2S were used as supporting electrolyte and sacrificial reagent to keep the stability of the C dots. Other supporting electrolytes including KNO_3, KCl, and NaOH and sacrificial reagents including methanol and ethanol were also used to investigate their influences on the PEC properties of the TNRA/C dot nanocomposites. Prior to the measurement, N_2 was purged into the electrolyte for 20 min to remove O_2. A 300 W Xe lamp (Beijing NBET Technology Co., Ltd.) was used as light source (100 mW/cm^2). Incident photon to current conversion efficiency (IPCE) was measured under monochromatic light, which was realized by the Xe lamp illuminating through a monochromator. The illumination intensity of the monochromatic light was measured by a luminometer. Impedance spectra were carried out in the dark and under illumination at 0 V vs Ag/AgCl in the frequency range of 0.1–10^5 Hz with AC voltage of 10 mV.

3. RESULTS AND DISCUSSION

Figure 1a shows the UV–vis absorption spectrum of as prepared C dots. Two peaks at around 236 and 340 nm are found, which may be attributed to the π–π^* transition.[22] The insets in Figure 1a depict the solutions of C dots under lamplight and UV light, and obviously, a blue light emission was

dx.doi.org/10.1021/am4059183 | ACS Appl. Mater. Interfaces 2014, 6, 4883–4890

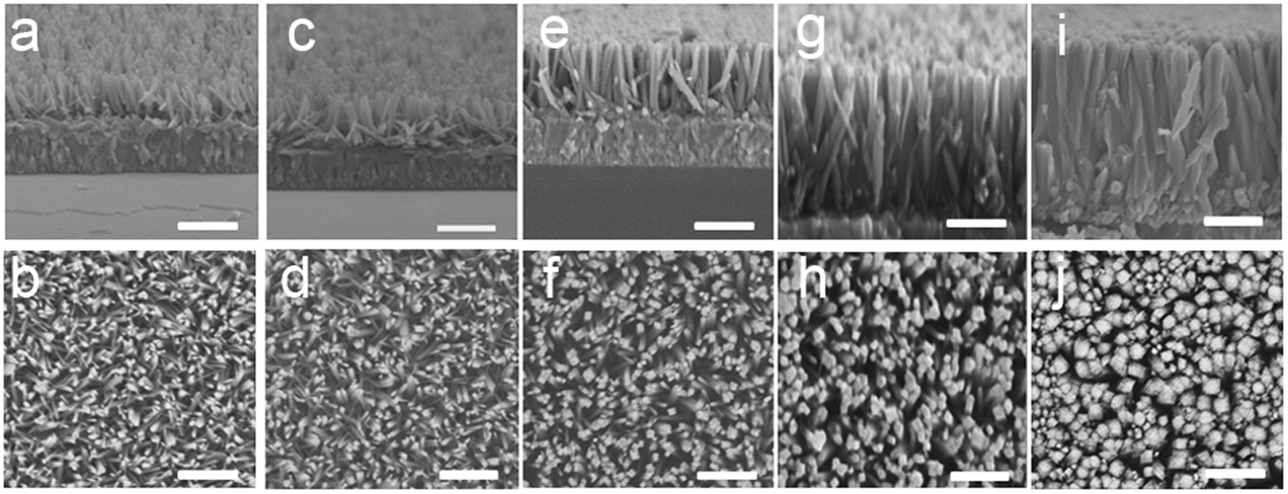

Figure 2. Cross sectional and top-view SEM images of TNRA growing for 3 h (a, b), 5 h (c, d), 6 h (e, f), 9 h (g, h), and 12 h (i, j). The scale bars are 1 μm.

observed under UV light excitation. Figure 1b shows the HRTEM image of C dots. Some of the C dots show the lattice fringes with interplane distance of about 0.34 nm, corresponding to the (002) distance of graphitic carbon,[24,36] and the amorphous C dots without obvious lattice fringes are also observed. By randomly measuring the size of 100 C dots, the size of the C dots is calculated to be 3.3 ± 0.4 nm. Excitation-dependent photoluminescence (PL) spectra of the C dots are given in Figure 1c. It indicates that the photoexcited charge carriers can be generated by the visible light. This phenomenon is attributed to their complex surface states.[26,37,38] To demonstrate the C dots loading on the surface of TNRA, XPS spectrum of TNRA/C dot nanocomposites was measured. Typical peaks of C dots (Figure 1d) and TiO_2 (Figure S1, Supporting Information) were detected, indicating successful loading of C dots on the surface of TNRA. From the C1s peaks, three peaks corresponding to C−C, C−N, and C═O were fitted at 284.6, 285.9, and 288.1 eV, respectively,[39] and no Ti−C bond was found in Figure S1, Supporting Information, indicating that the C dots were physically adsorbed on the surface of TNRA.

TNRA with different lengths were obtained by controlling the growth time at 150 °C. Figure 2a−j shows the top-down and cross section morphology of TNRA growing for 3, 5, 6, 9, and 12 h, separately. The corresponding average lengths of the TNRA were measured to be about 0.66, 1.0, 1.3, 2.3, and 3.2 μm. It is also found that the diameter of the TNRA increases as they grow for longer time. XRD pattern (Figure S2, Supporting Information) shows that the TNRA are oriented to the [001] direction, which is in good accordance with a previous report.[9]

Figure 3a,b shows the typical HRTEM images of TNRA/C dot nanocomposites. Obvious C dots on the edge of the TiO_2 nanorod (Figure 3a) and the lattice fringe with the direction different from that of the TiO_2 phase (Figure 3b) are observed, indicating that the C dots are successfully loaded on the surface of the TiO_2 nanorod. The Raman spectra of the C dots and the TNRA/C dot nanocomposites are shown in Figure 4. No obvious D band at 1353 cm^{-1} and G band at 1586 cm^{-1} are observed maybe due to the low intensity.[28] The peaks centered at 447 and 612 cm^{-1} are attributed to the rutile TiO_2 phase.[40]

To study the photoanodic activity of the TNRA/C dot nanocomposites dependence on the C dot loading, TNRA with

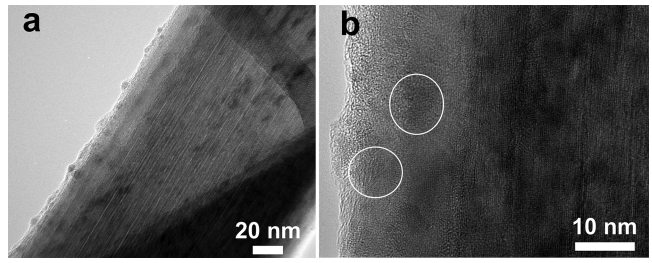

Figure 3. (a, b) HRTEM images of C dots on the surface of TiO_2 nanorod. The circles in (b) highlight the lattice fringes of C dots.

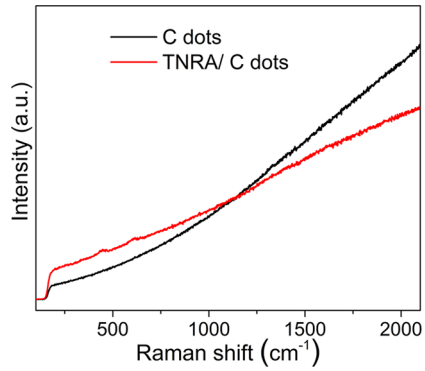

Figure 4. Raman spectra of C dots and TNRA/C dot nanocomposites.

the length of 0.66 μm were immersed into C dot solutions with different concentrations. Figure 5a shows the light absorption spectra of the bare TNRA and TNRA/C dot nanocomposites. Remarkable absorption plus scattering enhancement in the visible range can be observed when the concentration of C dots is 0.2 mg/mL. Further increase in the C dot concentration only slightly improves the light absorption plus scattering. This phenomenon reveals that the loading of the C dots on the surface of TNRA are nearly saturated.

Photocurrent density versus potential curves of the TNRA/C dot nanocomposites in Figure 5b shows that the photocurrent density is enhanced with increasing C dot loading until 0.4 mg/mL and then decreases with further increase of the C dot loading. The enhancement in photocurrent demonstrates that the C dots are good sensitizers for TiO_2, and photoexcited

dx.doi.org/10.1021/am4059183 | ACS Appl. Mater. Interfaces 2014, 6, 4883−4890

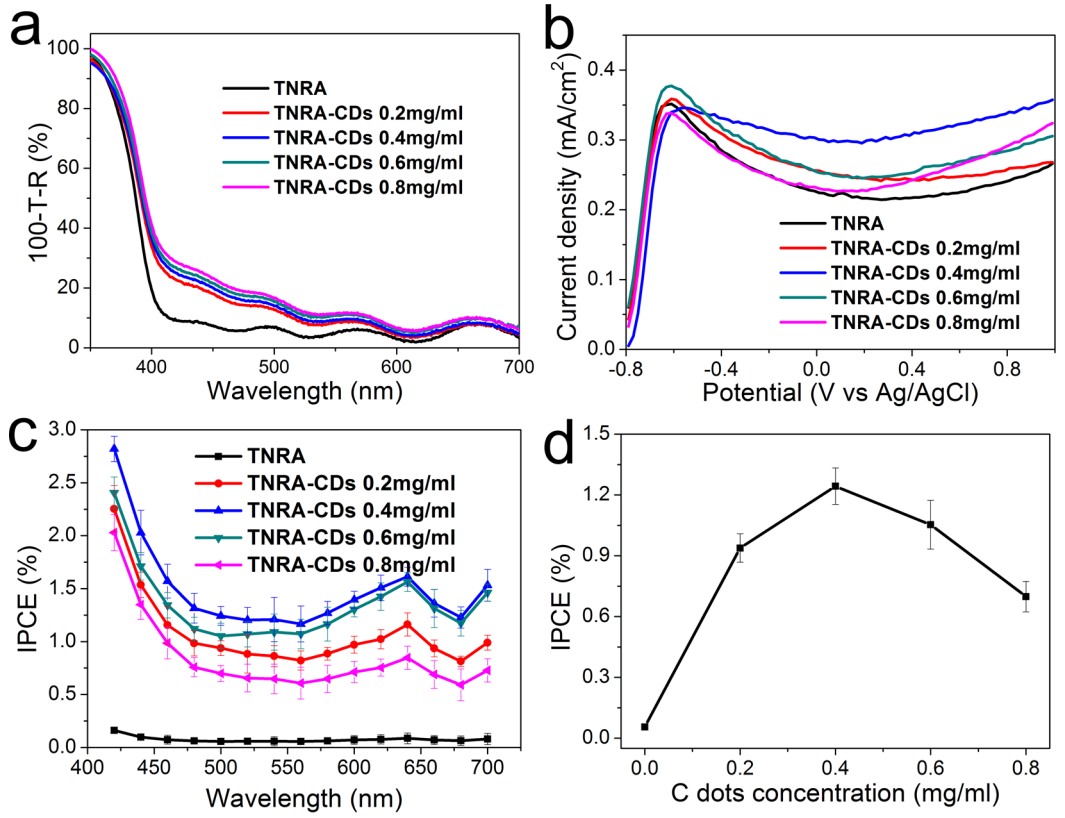

Figure 5. (a) 100-transmission-reflection (%) spectra, (b) photocurrent density versus potential curves, and (c) IPCE curves of TNRA/C dot nanocomposites. The nanocomposites were obtained through immersing the TNRA (0.66 μm) into C dot solutions with concentrations of 0.2, 0.4, 0.6, and 0.8 mg/mL. (d) Curve of IPCE at 500 nm versus C dot concentration.

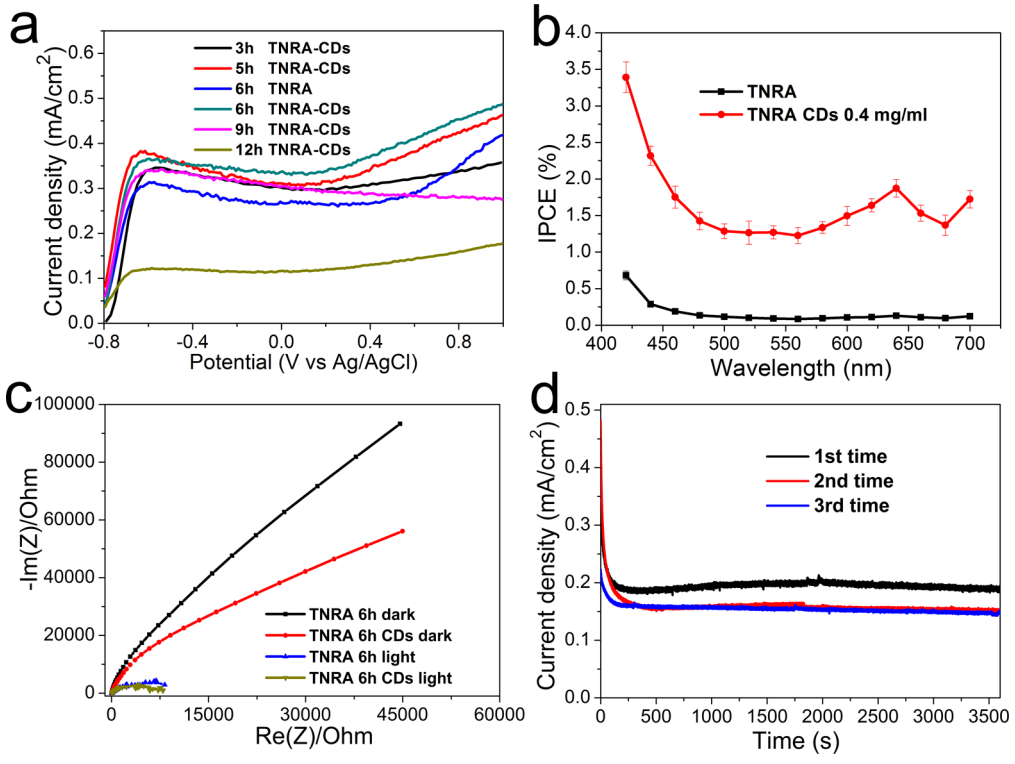

Figure 6. (a) Curves of photocurrent density versus growing time of the TNRA/C dots. The TNRA growth for different times was immersed into 0.4 mg/mL C dot solution. (b) IPCE plot of TNRA growing for 6 h with and without C dot loading. (c) Nyquist plot curves of TNRA and TNRA/C dot nanocomposites measured in the dark and under light. (d) Photocurrent densities of TNRA/C dots running for 1 h for three times.

dx.doi.org/10.1021/am4059183 | ACS Appl. Mater. Interfaces 2014, 6, 4883−4890

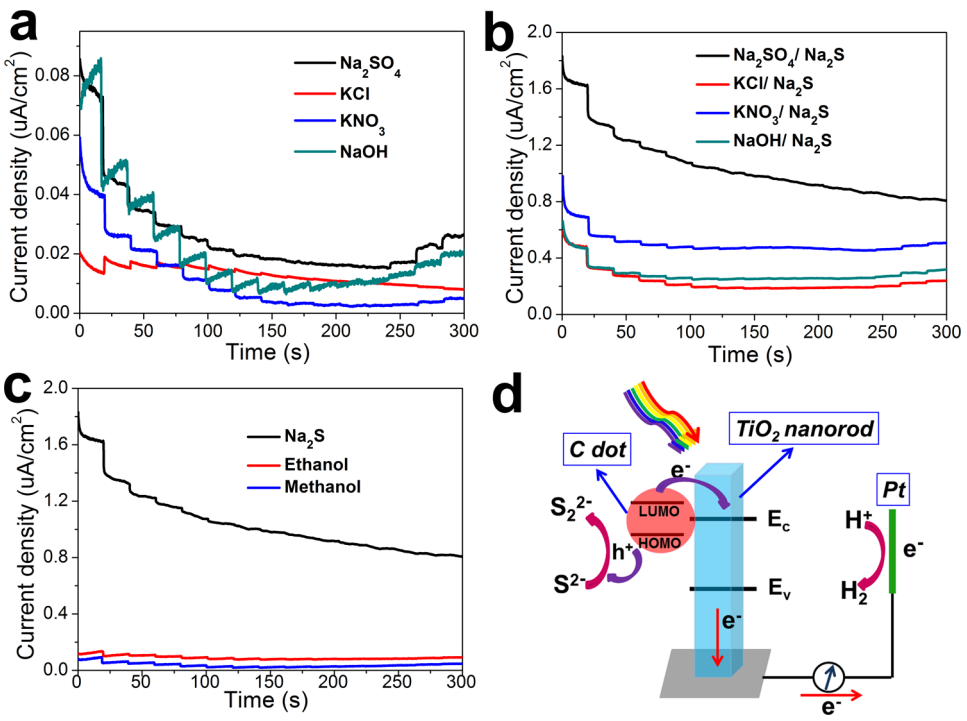

Figure 7. Photocurrent densities of TNRA/C dots measured under different monochromatic light in (a) different supporting electrolytes, (b) different supporting electrolytes with Na_2S as sacrificial reagent, and (c) different sacrificial reagents with $NaSO_4$ as supporting reagent. The monochromatic light from 420 to 700 nm is used with an increase of 20 nm/20s. (d) Mechanism of C dots in PCE properties enhancement of TNRA.

charge carriers can be transferred to TNRA and collected. Considering the continuous increase in light absorption with increasing the C dot concentration, the decrease in the enhancement may be attributed to the C dot aggregation on the surface of TNRA.[41,42] As the concentration of the C dots further increases, more C dot aggregations are formed on the surface of TNRA due to their surface functional groups like carboxyl and amido,[26] and photoexcited charge carriers recombine at the boundary of the C dots, leading to the decrease of the photocurrent density.[41,42] It is noted that, when the bias is more negative than −0.6 V, the change of the photocurrent densities is different from that under the bias more positive than −0.6 V. It may be caused by the more negative potential of −0.6 V. Further investigation is needed to clarify the phenomenon.

To further evaluate the PEC properties of the TNRA/C dot nanocomposites, IPCE spectra were measured versus incident light wavelength under monochromatic light. Calculation of the IPCE referred to the following equation:

$$\mathrm{IPCE} = 1240I/(\lambda J_{\mathrm{light}})$$

where I, λ, and J_{light} are photocurrent density, wavelength of incident light, and illumination intensity, respectively.[35] As shown in Figure 5c, it is evident that the IPCE is enhanced in the visible range, indicating that the incorporation of C dots remarkably improves the photoresponse of the TiO_2-based PEC cells in the visible range. It should also be noted that the IPCE values in the visible light range are different from one to another, especially at 600−700 nm. This phenomenon may be attributed to the complex surface states affecting the band gap of the C dots.[26,37] The IPCEs of TNRA/C dots illuminated under 500 nm are plotted versus the C dot concentrations in Figure 5d. The IPCE first increases until 0.4 mg/mL and then decreases, which is well consistent with the change in the photocurrent densities under potential more positive than −0.6 V.

For the photogenerated electrons collection, the electrons should transport across the TNRA along the axial direction. Therefore, the effect of TNRA length on the photoresponse of the TNRA C dots nanocomposites is also studied, as shown in Figure 6a. It is found that the photocurrent density is increasingly enhanced when the length of the TNRA changes from 0.68 to 1.3 μm. Then, a photocurrent density decrease is observed. This phenomenon is a compromise between the charge generation and charge collection. At first, with the increase in the length of TNRA to 1.3 μm, more C dots are loaded on the surface of the TNRA assuming that the density of the C dots on unit area of TNRA is identical. The increased C dot loading raises the photocurrent density. As the length increases from 1.3 to 2.3 μm, although more C dots are loaded, the increase in the length plays a major role. The charge carriers generated in the topper part of the TNRA should diffuse a longer distance to reach the FTO film, and the recombination rates of the charge carriers during the transport are largely increased, leading to the decrease of the photocurrent density.[5] Among the samples, the TNRA (1.3 μm) immersed in 0.4 mg/mL C dots have the best PEC performance. The photocurrent density is enhanced about 25.2% compared with the bare TRNA under the bias potential of 0 V. Their IPCE is shown in Figure 6b. The IPCE values in the range of 420 to 700 nm are 1.2−3.4%.

Impedance spectroscopy is a powerful tool to characterize the electric properties of semiconductor nanocomposites and has been widely employed in PEC systems, and the diameter of the Nyquist plot reflects the charge transfer resistance between the electrode and electrolyte.[43,44] Figure 6c presents a

dx.doi.org/10.1021/am4059183 | ACS Appl. Mater. Interfaces 2014, 6, 4883−4890

decreased semicircle diameter after the loading of C dots measured in the dark and under illumination, confirming that the C dots can enhance the carrier mobility at the interface of TNRA and electrolyte. Figure 6d shows the photocurrent density of the TNRA/C dot nanocomposites running for 3 times as the photoanode. It is found that the photocurrent density exhibits a slight decrease in the second time and is nearly stable in the third time. This degeneration may be caused by the partly detached C dots from the surface of TNRA due to the poor adhesion force. The stability of the TNRA/C dots should be improved. In situ growth of C dots on the surface of TNRA will be carried out in the future work.

To investigate the influence of the supporting electrolyte on the PEC performance of the TNRA/C dots nanocomposites, photocurrent densities are measured in other electrolytes including KNO_3, KCl, and NaOH. It is found that, without the sacrificial reagent, the photocurrent densities measured by using the electrolytes including Na_2SO_4, KNO_3, KCl, and NaOH are about 2 orders of magnitude smaller than that measured with sacrificial reagent, as shown in Figure 7a,b. Hence, it is confirmed that the HOMO of the C dots is higher than the water oxidation potential, which blocks the flow of the photogenerated holes from C dots to the solution. Without using Na_2S as sacrificial reagent, the holes will accumulate in the HOMO of C dots as a result of small photocurrent due to the large electron−hole recombination rate. The differences of the photocurrent densities among different electrolytes may be caused by the different conductivities of different anions and changed surface states by the interactions between the anions and the surface functional groups of C dots.[26,37] Moreover, other frequently used sacrificial reagents like ethanol and methanol are also investigated,[45] as shown in Figure 7c. It is found that Na_2S is the best sacrificial reagent. It indicates that the Na_2S is more easily oxidized than ethanol and methanol, well consistent with the previous report.[45]

On the basis of the aforementioned analysis, a possible mechanism for the C dots enhancement in PEC properties of TNRA was proposed, as shown in Figure 7d. When excited by the visible light, the electrons in the HOMO level of the C dots get enough energy and jump to the LUMO level of the C dots. Then, they are transferred to the conduction band of TiO_2. After that, the electrons are transported through the TiO_2 nanorod and FTO film. Afterward, the electrons are conducted through the external circuit to the counter electrode and react with H^+ to form H_2. The holes left in the HOMO of C dots react with the S^{2-} to form S_2^{2-}.[4]

The main advantages of C dots for its application in the PEC enhancement of TNRA are their elemental abundance, low cost, and low toxicity compared with the toxic metal-based quantum dots (CdSe, CdS, and PbS), expensive noble metals including Au, Ag, and Pt, and expensive dyes. However, the stability of the C dots needs further improvement, and the enhanced efficiency in the visible light range is still too low. Chemical doping and surface modifications are potential approaches to tune the surface states and band gap of the C dots.[46,47]

4. CONCLUSIONS

We demonstrated that the PCE properties of C dots decorated TNRA are dependent on the C dots loading and the length of TNRA. Photocurrent density curves showed that the photocurrent density reached a maximum when concentration of C dots was 0.4 mg/mL, and a further increase in the C dots concentration decreased the photocurrent, which may be caused by the surface aggregation of C dots. A compromise existed between charge transport and charge collection as the TNRA length increased. The IPCEs of the TNRA/C dots nanocomposites in the visible range were up to 1.2−3.4% by immersing the TNRA (1.3 μm) in 0.4 mg/mL C dots solution. Impedance spectroscopy confirmed that the incorporation of C dots on the surface of TNRA can improve the charge transfer process between the electrode and electrolyte. Na_2SO_4 is a better choice of supporting electrolyte compared with KNO_3, KCl, and NaOH, and Na_2S is better than ethanol and methanol as sacrificial reagent. This work can serve as a guidance for the design of highly efficient photoanode for PEC cells based on TNRA/C dot nanocomposites.

■ ASSOCIATED CONTENT

Supporting Information

XPS spectrum and XRD pattern of TiO_2 nanorod arrays with a growth time of 9 h. This information is available free of charge via the Internet at http://pubs.acs.org.

■ AUTHOR INFORMATION

Corresponding Author

*E-mail: aprqz@cityu.edu.hk. Tel: +852 3442 7849. Fax: +852 3442 0538.

Author Contributions

The manuscript was written through contributions of all authors. All authors have given approval to the final version of the manuscript.

Notes

The authors declare no competing financial interest.

■ ACKNOWLEDGMENTS

The work described in this paper is supported in part by a grant from the Research Grants Council of Hong Kong SA [Project No. CityU 103812]. We are grateful to Professor Andrey L. Rogach, Dr. Chunyi Zhi, Dr. Yu Wang, and Dr. Sergii Kalytchuk for their help with the experiment.

■ REFERENCES

(1) Fujishima, A.; Honda, H. Electrochemical Photolysis of Water at a Semiconductor Electrode. *Nature* **1972**, *238*, 37−38.

(2) Gratzel, M. Photoelectrochemical Cells. *Nature* **2001**, *414*, 338−344.

(3) Khan, S. U. M.; Al-Shahry, M.; Ingler, W. B. Efficient Photochemical Water Splitting by a Chemically Modified n-TiO_2. *Science* **2002**, *297*, 2243−2245.

(4) Leung, D. Y. C.; Fu, X.; Wang, C.; Ni, M.; Leung, M. K. H.; Wang, X.; Fu, X. Hydrogen Production over Titania-Based Photocatalysts. *ChemSusChem* **2010**, *3*, 681−694.

(5) Hwang, Y. J.; Hahn, C.; Liu, B.; Yang, P. Photoelectrochemical Properties of TiO_2 Nanowire Arrays: A Study of the Dependence on Length and Atomic Layer Deposition Coating. *ACS Nano* **2012**, *6*, 5060−5069.

(6) Walter, M. G.; Warren, E. L.; McKone, J. R.; Boettcher, S. W.; Mi, Q.; Santori, E. A.; Lewis, N. S. Solar Water Splitting Cells. *Chem. Rev.* **2010**, *110*, 6446−6473.

(7) Cho, I. S.; Lee, C. H.; Feng, Y.; Logar, M.; Rao, P. M.; Cai, L.; Kim, D. R.; Sinclair, R.; Zheng, X. Codoping Titanium Dioxide Nanowires with Tungsten and Carbon for Enhanced Photoelectrochemical Performance. *Nat. Commun.* **2013**, *4*, 1723−1730.

(8) Enache-Pommer, E.; Boercker, J. E.; Aydil, E. S. Electron Transport and Recombination in Polycrystalline TiO_2 Nanowire Dye-Sensitized Solar Cells. *Appl. Phys. Lett.* **2007**, *91*, 123116.

(9) Liu, B.; Aydil, E. S. Growth of Oriented Single-Crystalline Rutile TiO_2 Nanorods on Transparent Conducting Substrates for Dye-Sensitized Solar Cells. *J. Am. Chem. Soc.* **2009**, *131*, 3985−3990.
(10) Mor, G. K.; Shankar, K.; Paulose, M.; Varghese, O. K.; Grimes, C. A. Use of Highly-Ordered TiO_2 Nanotube Arrays in Dye-Sensitized Solar Cells. *Nano Lett.* **2006**, *6*, 215−218.
(11) Zhu, K.; Neale, N. R.; Miedaner, A.; Frank, A. J. Enhanced Charge-Collection Efficiencies and Light Scattering in Dye-Sensitized Solar Cells Using Oriented TiO_2 Nanotubes Arrays. *Nano Lett.* **2007**, *7*, 69−74.
(12) Wang, Y.; Zhang, Y.-Y.; Tang, J.; Wu, H.; Xu, M.; Peng, Z.; Gong, X.-G.; Zheng, G. Simultaneous Etching and Doping of TiO_2 Nanowire Arrays for Enhanced Photoelectrochemical Performance. *ACS Nano* **2013**, *7*, 9375−9383.
(13) Sayed, F. N.; Jayakumar, O. D.; Sasikala, R.; Kadam, R. M.; Bhatadwaj, R.; Kienle, L.; Schurmann, U.; Kaps, S.; Adelung, R.; Mittal, J. P.; Tyagi, A. K. Photochemical Hydrogen Generation Using Nitrogen-Doped TiO_2 − Pd Nanoparticles: Facile Synthesis and Effect of Ti^{3+} Incorporation. *J. Phys. Chem. C* **2012**, *116*, 12462−12467.
(14) Tanaka, A.; Sakaguchi, S.; Hashimoto, K.; Kominami, H. Preparation of Au/TiO_2 with Metal Cocatalysts Exhibiting Strong Surface Plasmon Resonance Effective for Photoinduced Hydrogen Formation under Irradiation of Visible Light. *ACS Catal.* **2013**, *3*, 79−85.
(15) Pu, Y.-C.; Wang, G.; Chang, K.-D.; Ling, Y.; Lin, Y.-K.; Fitzmorris, B. C.; Liu, C.-M.; Lu, X.; Tong, Y.; Zhang, J. Z.; Hsu, Y.-J. Au Nanostructure-Decorated TiO_2 Nanowires Exhibiting Photoactivity across Entire UV-Visible Region for Photoelectrochemical Water Splitting. *Nano Lett.* **2013**, *13*, 3817−3823.
(16) Awazu, K.; Fujimaki, M.; Rockstuhl, C.; Tominaga, J.; Murakami, H.; Ohki, Y.; Yoshida, N.; Watanabe, T. A Plasmonic Photocatalyst Consisting of Silver Nanoparticles Embedded in Titanium Dioxide. *J. Am. Chem. Soc.* **2008**, *130*, 1676−1680.
(17) Bessekhouad, Y.; Robert, D.; Weber, J.-V. Photocatalytic Activity of Cu_2O/TiO_2, Bi_2O_3/TiO_2 and $ZnMn_2O_4/TiO_2$ Heterojunctions. *Catal. Today* **2005**, *101*, 315−321.
(18) Jang, W.; Kim, D.; Kim, J.; Min, B. K.; Kim, J.-D.; Yoo, K. Uniform Decoration of Linker-Free Quantum Dots onto Mesoporous TiO_2 Using Liquid Carbon Dioxide. *Chem. Mater.* **2010**, *22*, 4350−4352.
(19) Lee, Y.-L.; Chi, C.-F.; Liau, S.-Y. CdS/CdSe Co-Sensitized TiO_2 Photoelectrode for Efficient Hydrogen Generation in a Photoelectrochemical Cell. *Chem. Mater.* **2010**, *22*, 922−927.
(20) Hensel, J.; Wang, G.; Li, Y.; Zhang, J. Z. Synergistic Effect of CdSe Quantum Dot Sensitization and Nitrogen Doping of TiO_2 Nanostructures for Photoelectrochemical Solar Hydrogen Generation. *Nano Lett.* **2010**, *10*, 478−483.
(21) Zhang, J.; Du, P.; Schneider, J.; Jarosz, P.; Eisenberg, R. Photogeneration of Hydrogen from Water Using an Integrated System Based on TiO_2 and Platinum(II) Diimine Dithiolate Sensitizers. *J. Am. Chem. Soc.* **2007**, *129*, 7726−7727.
(22) Jaiswal, A.; Ghosh, S. S.; Chattopadhyay, A. One Step Synthesis of C-Dots by Microwave Mediated Caramelization of Poly(ethylene Glycol). *Chem. Commun.* **2012**, *48*, 407−409.
(23) Baker, S. N.; Baker, G. A. Luminescent Carbon Nanodots: Emergent Nanolights. *Angew. Chem., Int. Ed.* **2010**, *49*, 6726−6744.
(24) Li, H.; He, X.; Kang, Z.; Huang, H.; Liu, Y.; Liu, J.; Lian, S.; Tsang, C. H. A.; Yang, X.; Lee, S.-T. Water-Soluble Fluorescent Carbon Quantum Dots and Photocatalyst Design. *Angew. Chem., Int. Ed.* **2010**, *49*, 4430−4434.
(25) Liu, H.; Ye, T.; Mao, C. Fluorescent Carbon Nanoparticles Derived from Candle Soot. *Angew. Chem., Int. Ed.* **2007**, *46*, 6473−6475.
(26) Zhu, S.; Meng, Q.; Wang, L.; Zhang, J.; Song, Y.; Jin, H.; Zhang, K.; Sun, H.; Wang, H.; Yang, B. Highly Photoluminescent Carbon Dots for Multicolor Patterning, Sensors, and Bioimaging. *Angew. Chem., Int. Ed.* **2013**, *52*, 3953−3957.
(27) Zhu, S.; Tang, S.; Zhang, J.; Yang, B. Control the Size and Surface Chemistry of Graphene for the Rising Fluorescent Materials. *Chem. Commun.* **2012**, *48*, 4527−4539.
(28) Fang, Y.; Guo, S.; Li, D.; Zhu, C.; Ren, W.; Dong, S.; Wang, E. Easy Synthesis and Imaging Applications of Cross-Linked Green Fluorescent Hollow Carbon Nanoparticles. *ACS Nano* **2012**, *6*, 400−409.
(29) Zhang, X.; Zhang, Y.; Wang, Y.; Kalytchuk, S.; Kershaw, S. V; Wang, Y.; Wang, P.; Zhang, T.; Zhao, Y.; Zhang, H.; Cui, T.; Wang, Y.; Zhao, J.; Yu, W. W.; Rogach, A. L. Color-Switchable Electroluminescence of Carbon Dot Light-Emitting Diodes. *ACS Nano* **2013**, *7*, 11234−11241.
(30) Gupta, V.; Chaudhary, N.; Srivastava, R.; Sharma, G. D.; Bhardwaj, R.; Chand, S. Luminscent Graphene Quantum Dots for Organic Photovoltaic Devices. *J. Am. Chem. Soc.* **2011**, *133*, 9960−9963.
(31) Tang, D.; Zhang, H.; Huang, H.; Liu, R.; Han, Y.; Liu, Y.; Tong, C.; Kang, Z. Carbon Quantum Dots Enhance the Photocatalytic Performance of $BiVO_4$ with Different Exposed Facets. *Dalton Trans.* **2013**, *42*, 6285−6289.
(32) Zhuo, S.; Shao, M.; Lee, S.-T. Upconversion and Down-conversion Fluorescent Graphene Quantum Dots: Ultrasonic Preparation and Photocatalysis. *ACS Nano* **2012**, *6*, 1059−1064.
(33) Zhang, H.; Huang, H.; Ming, H.; Li, H.; Zhang, L.; Liu, Y.; Kang, Z. Carbon Quantum dots/Ag_3PO_4 Complex Photocatalysts with Enhanced Photocatalytic Activity and Stability under Visible Light. *J. Mater. Chem.* **2012**, *22*, 10501−10506.
(34) Li, H.; Liu, R.; Liu, Y.; Huang, H.; Yu, H.; Ming, H.; Lian, S.; Lee, S.-T.; Kang, Z. Carbon Quantum dots/Cu_2O Composites with Protruding Nanostructures and Their Highly Efficient (near) Infrared Photocatalytic Behavior. *J. Mater. Chem.* **2012**, *22*, 17470−17475.
(35) Guo, C. X.; Dong, Y.; Yang, H. B.; Li, C. M. Graphene Quantum Dots as a Green Sensitizer to Functionalize ZnO Nanowire Arrays on F-Doped SnO_2 Glass for Enhanced Photoelectrochemical Water Splitting. *Adv. Energy Mater.* **2013**, *3*, 997−1003.
(36) Liu, J.; Shao, M.; Chen, X.; Yu, W.; Liu, X.; Qian, Y. Large-Scale Synthesis of Carbon Nanotubes by an Ethanol Thermal Reduction Process. *J. Am. Chem. Soc.* **2003**, *125*, 8088−8089.
(37) Shang, J.; Ma, L.; Li, J.; Ai, W.; Yu, T.; Gurzadyan, G. G. The Origin of Fluorescence from Graphene Oxide. *Sci. Rep.* **2012**, *2*, 792.
(38) Sun, Y.-P.; Zhou, B.; Lin, Y.; Wang, W.; Shiral Fernando, K. A.; Pathak, P.; Meziani, M. J.; Harruff, B. A.; Wang, X.; Wang, H.; Luo, P. G.; Yang, H.; Kose, M. E.; Chen, B.; Monica Veca, L.; Xie, S.-Y. Quantum-Sized Carbon Dots for Bright and Colorful Photoluminescence. *J. Am. Chem. Soc.* **2006**, *128*, 7756−7757.
(39) Liu, S.; Tian, J.; Wang, L.; Zhang, Y.; Qin, X.; Luo, Y.; Asiri, A. M.; Al-Youbi, A. O.; Sun, X. Hydrothermal Treatment of Grass: A Low-Cost, Green Route to Nitrogen-Doped, Carbon-Rich, Photoluminescent Polymer Nanodots as an Effective Fluorescent Sensing Platform for Label-Free Detection of Cu(II) Ions. *Adv. Mater.* **2012**, *24*, 2037−2041.
(40) Swamy, V.; Muddle, B. C.; Dai, Q. Size-Dependent Modifications of the Raman Spectrum of Rutile TiO_2. *Appl. Phys. Lett.* **2006**, *89*, 163118.
(41) Shalom, M.; Buhbut, S.; Tirosh, S.; Zaban, A. Design Rules for High-Efficiency Quantum-Dot-Sensitized Solar Cells: A Multilayer Approach. *J. Phys. Chem. Lett.* **2012**, *3*, 2436−2441.
(42) Kamat, P. V. Boosting the Efficiency of Quantum Dot Sensitized Solar Cells through Modulation of Interfacial Charge Transfer. *Acc. Chem. Res.* **2012**, *45*, 1906−1915.
(43) Ye, M.; Gong, J.; Lai, Y.; Lin, C.; Lin, Z. High-Efficiency Photoelectrocatalytic Hydrogen Generation Enabled by Palladium Quantum Dots-Sensitized TiO_2 Nanotube Arrays. *J. Am. Chem. Soc.* **2012**, *134*, 15720−15723.
(44) Liu, H.; Cheng, S.; Wu, M.; Wu, H.; Zhang, J.; Li, W.; Cao, C. Photoelectrocatalytic Degradation of Sulfosalicylic Acid and Its Electrochemical Impedance Spectroscopy Investigation. *J. Phys. Chem. A* **2000**, *104*, 7016−7020.

(45) Schneider, J.; Bahnemann, D. W. Undesired Role of Sacrificial Reagents in Photocatalysis. *J. Phys. Chem. Lett.* **2013**, *4*, 3479−3483.
(46) Jin, S. H.; Kim, D. H.; Jun, G. H.; Hong, S. H.; Jeon, S. Tuning the Photoluminescence of Graphene Quantum Dots through the Charge Transfer Effect of Functional Groups. *ACS Nano* **2013**, *7*, 1239−1245.
(47) Liu, H.; Liu, Y.; Zhu, D. Chemical Doping of Graphene. *J. Mater. Chem.* **2011**, *21*, 3335−3345.